Changes in 5*d* Band Polarization in Rare-Earth Compounds

S. Langridge,[1,2,*] J. A. Paixão,[3] N. Bernhoeft,[1,4] C. Vettier,[1] G. H. Lander,[2] Doon Gibbs,[5] S. Aa. Sørensen,[6] A. Stunault,[1] D. Wermeille,[1] and E. Talik[7]

[1]*European Synchrotron Radiation Facility, B.P. 220X, F-38043 Grenoble, France*
[2]*European Commission, JRC, Institute for Transuranium Elements, Postfach 2340, D-76125 Karlsruhe, Germany*
[3]*Departamento de Fisica, University of Coimbra, P-3000 Coimbra, Portugal*
[4]*Institut Laue Langevin, B.P. 156X, F-38042 Grenoble, France*
[5]*Physics Department, Brookhaven National Laboratory, Upton, New York 11973*
[6]*Solid State Physics Department, Risø National Laboratory, DK-4000 Roskilde, Denmark*
[7]*Institute of Physics, University of Silesia, Katowice, Poland*

(Received 28 May 1998)

X-ray resonant magnetic scattering has been used to examine the magnetic interactions coupling the rare earth and iron sublattices in the antiferromagnetic compound $DyFe_4Al_8$. Dramatic differences are observed in the temperature dependencies of the energy profiles at resonance depending on whether the photon energy is tuned to the Dy L_2 or L_3 absorption edge. In particular, for temperatures increasing from 10 K, the resonant scattering intensity at the L_3 edge decreases whereas that at the L_2 edge rises. We suggest a physical model capable of reproducing these phenomena. [S0031-9007(99)08671-8]

PACS numbers: 75.25.+z, 75.30.Mb

The $4f$ electrons of the rare-earth elements are well shielded from their environment so that the interactions among them take place mainly through their coupling to the $5d$ electrons, which form the major constituent of the conduction-electron band [1]. Interesting properties are found when the rare earths are combined in compounds, multilayers, or amorphous melts with $3d$-transition elements. Broadly speaking, the $3d$ elements tend to give rise to a higher magnetic-ordering temperature, whereas the rare-earth elements introduce magnetic anisotropy. The magnetic nature of the rare-earth $5d$ states is crucial to an understanding of this class of materials. In this Letter, we report results of resonant magnetic x-ray scattering (XRES) experiments on a single crystal of $DyFe_4Al_8$ that give new insight into how the $5d$ conduction band is affected on cooling below the Néel temperature T_N, first by the ordering of the Fe $3d$ electrons, and then by the subsequent growth of the ordered component of the Dy $4f$ moments. The experiments were performed by monitoring the intensity and energy dependence of the resonant magnetic scattering for incident photon energies tuned near the Dy L_2 and L_3 edges as a function of temperature.

The compound $DyFe_4Al_8$ crystallizes with the body-centered tetragonal $ThMn_{12}$ structure [see Fig. 1(a)], with $a = b = 8.74$ Å, and $c = 5.036$ Å. Neutron-diffraction experiments [2] have shown that the single crystal used in our investigation has ordered Fe and Al sublattices. Whereas the Dy atoms contribute to all Bragg reflections, the lower symmetry of the Fe atomic sites imposes more restrictive diffraction conditions, allowing the contributions of the Dy and Fe sublattices to be separated [3]. Much work has been done on the ordered MFe_4Al_8 compounds (M = rare earth or actinide). Early studies [4] showed that antiferromagnetic (AF) ordering occurred between 140 and 180 K depending on the atom species. Our neutron experiments [2] show that the Fe sublattice orders with the moments in the (001) plane at $T_N \sim 170$ K in a small modification of the G-type AF structure [5]. Superimposed on the AF order, shown in Fig. 1(a), is a long-wavelength modulation with $\mathbf{q} = [qq0]$, where $q \sim 0.14$ reciprocal lattice units (rlu) at T_N and locks to $q = 0.1333 = \frac{2}{15}$ rlu below $\sim$100 K. At a lower temperature, which we define as T_{Dy} ($\sim$50 K), the intensities of the neutron reflections start to change indicative of a progressive (with decreasing temperature) ordering of the Dy $4f$ moment. T_{Dy} also heralds the onset of a hyperfine field in the Mössbauer spectroscopy of ^{161}Dy in this compound [6]. No other phase transitions have been observed by us or earlier workers [4–6].

Synchrotron experiments on a single crystal of $DyFe_4Al_8$, with a polished face (1×1 mm^2), were first performed at the bending magnet beam line X22C at the National Synchrotron Light Source at Brookhaven National Laboratory. The XRES measurements were performed at AF satellites situated symmetrically around the charge reflections at $\pm\mathbf{q}$ in reciprocal space. At the L_3 absorption edge of Dy a maximum in intensity was observed at low temperature. On warming, it decreased rapidly at $\sim$25 K, however, interestingly, a small signal remained up to T_N. At T_{Dy} and below, we also observed the appearance of weak $2q$ charge satellites, indicating the presence of a magnetoelastic distortion that accompanies the ordering of the Dy $4f$ moments. The remaining experiments discussed in this paper were performed on the ID20 undulator beam line [7] of the European Synchrotron Radiation Facility, Grenoble, France. A double crystal, Si(111), monochromator selected the appropriate x-ray energy giving linearly σ-polarized radiation. This was then diffracted at the sample position onto a graphite crystal [(006) reflection], which was used

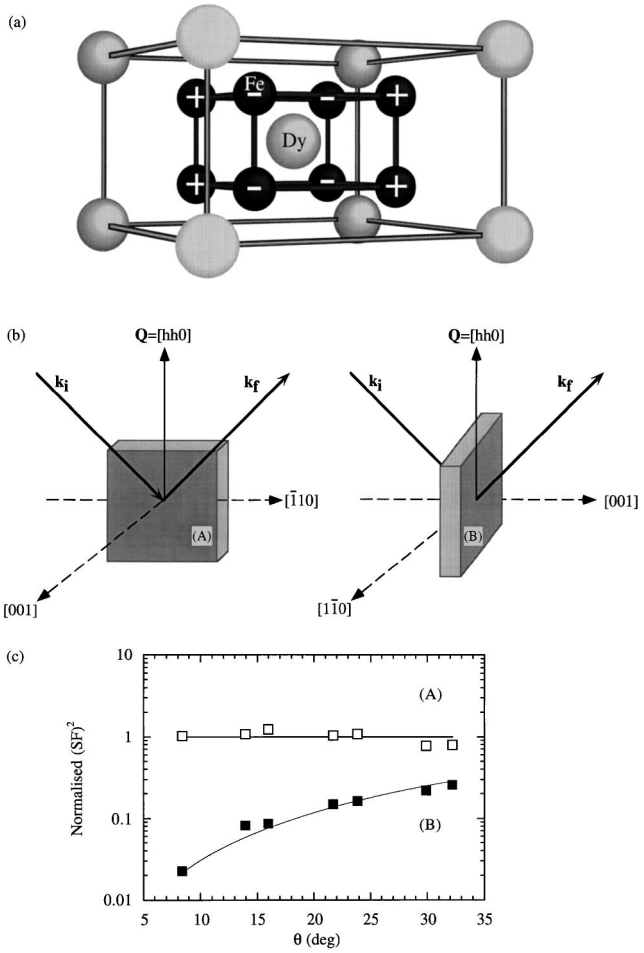

FIG. 1. (a) The $DyFe_4Al_8$ crystal structure (omitting the Al atoms) showing the Dy atom surrounded by eight Fe atoms. The + and − signs on the Fe atoms indicate the G-type antiferromagnetic structure. (b) The two configurations A and B used in the experiment. The momentum transfer is $\mathbf{Q} = [hh0] = 4\pi(\sin\theta/\lambda)$, where $\mathbf{k}_i$ and $\mathbf{k}_f$ are the incident and scattered wave vectors, respectively. The scattering angle is 2θ. As determined in these experiments, the magnetic moments rotate in the (001) plane—darkly shaded in the figure. (c) Lorentz-corrected intensity as a function of θ for configurations A and B at a temperature of 12 K. All are measured in the $\sigma \rightarrow \pi$ channel. The average value found for all of the satellite intensities in configuration A (open squares) has been normalized to 1. For configuration B (closed squares), the solid line is then drawn to predict the intensities with no adjustable parameter.

to discriminate the σ- and π-polarized components of the scattered radiation, corresponding to nonrotated and rotated channels, respectively. The sample could be rotated azimuthally about the scattering vector. Experiments aimed at resolving the magnetic structure at 12 K were performed at the Dy L_3 edge. The two configurations used, labeled A and B, are shown in Fig. 1(b) and the results are shown in Fig. 1(c).

To interpret these results, we note that the resonant signal observed at the L edges of the lanthanides may be described in terms of a multipole expansion. The leading terms involve the promotion of $2p$ core electrons to partially filled $5d$ and $4f$ band states via $E1$ (electric dipole) and $E2$ (electric quadrupole) transitions, respectively [8–10]. The observed energy spectra appear to peak at positions consistent with an $E1$ transition [11] and depend directly on the polarization of the $5d$ bands. An important point is that we have been unable to detect any significant intensity associated with $E2$ transitions, which may be identified by their angular and polarization dependencies [12]. The null result of a special search for such $E2$ intensity performed in the B configuration with $\sigma \rightarrow \sigma$ geometry, in which the $E1$ signal is forbidden, leads us to conclude that any $E2$ contribution to the intensities is $<10\%$. However, the presence of $4f$ moments is nevertheless important. Similar experiments on the isostructural compound $LuFe_4Al_8$, which orders in a similar magnetic structure, found no measurable intensity at either of the Lu $L_{2,3}$ edges. Since the $4f$ shell in Lu is full (implying no net $4f$ moment), we infer that the presence of $4f$ moments in the Dy compound plays an important role even if the $E2$ resonance itself is weak.

The $E1$ cross section [12] in the σ to π channel has two components. One is parallel to $\mathbf{Q}$ and proportional to $(m_\parallel \sin\theta)^2$. The other is perpendicular to $\mathbf{Q}$ in the scattering plane and proportional to $(m_\perp \cos\theta)^2$, where $m_\parallel$ and $m_\perp$ are transition probabilities [8]. In configuration A [Fig. 1(b)] *both* components were observed. The fact that the scattering intensity is independent of θ suggests that $m_\parallel = m_\perp = m$, so that the scattered intensity is proportional to $(m_\parallel \sin\theta)^2 + (m_\perp \cos\theta)^2 = m^2$. In configuration B [Fig. 1(b)] only the $(m_\parallel \sin\theta)^2$ component parallel to $\mathbf{Q}$ was observed, and the intensities follow a sinusoidal dependence. These results are consistent with the structure having two equal components in the shaded plane of Fig. 1(b). Since the propagation vector is along $\mathbf{Q} = [110]$ within the scattering plane, the magnetic structure is a cycloid.

We now focus on the temperature dependence of the measured intensities (see Fig. 2), which is the most surprising part of our results. There are two remarkable features of the data to explain. First, the energy (and angular) integrated intensity of the XRES at the Dy L_3 edge *falls* for $12 < T < 25$ K, stays approximately constant up to $T \sim 100$ K, and then falls near T_N. In contrast, the intensity at the L_2 edge initially *rises*, for $12\ \text{K} < T < T_{\text{Dy}}$, and then also falls smoothly to T_N. This effect generates a "temperature dependent" branching ratio (defined as the ratio of the integrated intensities at the L_3 to L_2 edges), shown in the inset of Fig. 2(a). Such an observation is unexpected, and, as far as we know, unprecedented in either scattering or dichroism experiments at rare-earth L edges. The second point is that these intensity changes are accompanied by significant shifts in line shape and center of mass of the resonance (see Fig. 3). We recall that all of the spectra have an essentially pure $E1$ character.

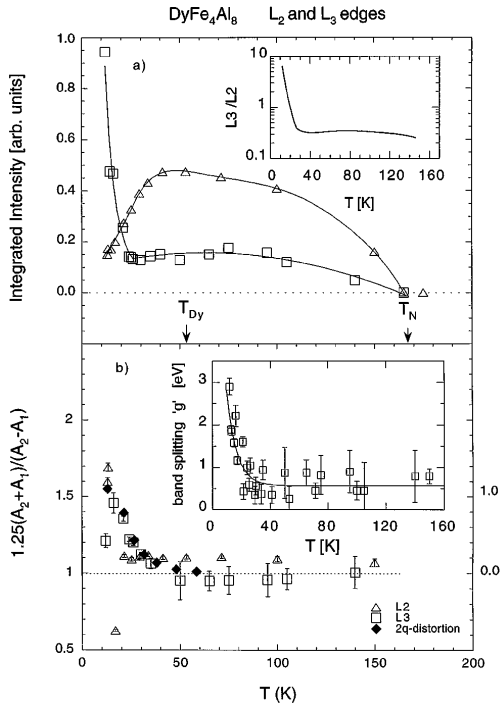

FIG. 2. (a) Temperature dependence of the energy integrated intensity of the (440) + q satellite in the $\sigma \rightarrow \pi$ channel as measured at the L_2 (open triangles) and L_3 (open squares) edges of dysprosium. These intensities have not been corrected for the small difference in absorption at the two edges. The lines through the points are a result of calculations using the model presented in the text. The derived temperature dependence of the branching ratio is shown in the inset. (b) and the corresponding inset show the temperature evolution of the parameters from the fits. The filled diamonds (right-hand scale) show the temperature dependence of the $2q$ charge amplitude (so identified as it is present only in the $\sigma \rightarrow \sigma$ channel), normalized at $T = 12$ K. The factor 1.25 in the left-hand scale is the normalization arising from a fractional hole occupation of $\frac{8}{10}$ for two electrons in the $5d$ band.

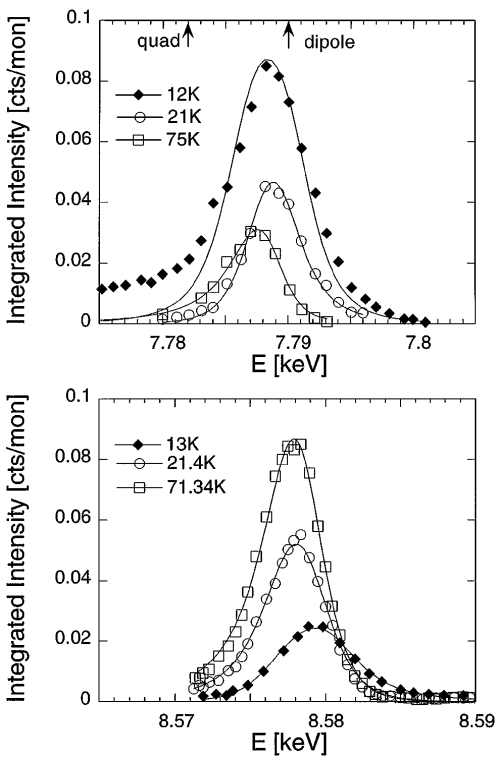

FIG. 3. The incident photon energy dependence of the angle-integrated scattering at the Dy L_3 (upper panel) and L_2 (lower panel) edges as measured at different temperatures at the (440) + q satellite in the $\sigma \rightarrow \pi$ channel. The solid lines result form the model described in the text. They reproduce both the energy and temperature dependence of the observations. There is only one overall scale factor for the upper and lower figures. The expected energies of the $E1$ (dipole) and $E2$ (quadrupole) transitions at the L_3 edge as given in Ref. [11] are marked in the upper panel.

Indeed, extensive modeling *assuming* the additional presence of either a strong nonresonant signal or an $E2$ signal or a combination of both has been unable to reproduce the temperature dependence of the line shapes.

To understand these effects, we need to go beyond the standard formalism of XRES. The symmetry embodied in the approximation of an isolated ion, which generates a temperature independent branching ratio, needs to be lowered. Specifically, one would like to add two "solid state" effects: that $DyFe_4Al_8$ is antiferromagnetic and that it is metallic. Accordingly, we have developed an elementary model of the XRES cross section in an antiferromagnetic metal. The minimal assumptions necessary are the following: (i) The antiferromagnetic state is considered to arise out of a single paramagnetic band which is split into two bands on doubling the unit cell below T_N. A parameter, $2g$, represents the rigid splitting of the bands labeled 1 and 2. The individual bands are not spin split, rather it is the preferential spatial distribution of the "up" and "down" spin electron (quasiparticle) density on the two magnetic sublattices which generates the antiferromagnetic state [13]. We write the probability of an electron being in the spin up or down lower band as $0.5(1 \pm \varepsilon_1)$. (ii) For small sublattice polarization, a linear correction for the up and down components, $(1 \pm \delta_1)$, may be made to the mean radial matrix element.

We define the probability of finding an electron in the lower band as a_1, and analogous quantities are defined for the upper band, subscript 2. In general, $\varepsilon_2 = -\varepsilon_1$. We start from the anomalous scattering amplitude [14] and consider transitions into the intermediate band states described under the approximations (i) and (ii) above. This gives the incident energy dependence of the cross section as

$$|f|^2 \propto \frac{A_1^2[\Gamma^2 + (E_0 - \hbar\omega_i + gA_2/A_1)^2]}{[(E_0 - \hbar\omega_i - g)^2 + \Gamma^2][(E_0 - \hbar\omega_i + g)^2 + \Gamma^2]},$$

where Γ is the width, E_0 is the pole of the resonance, ω_i is the incident photon frequency, $A_1 = (1 - a_1)(\varepsilon_1 + \delta_1) + (1 - a_2)(\varepsilon_2 + \delta_2)$, and $A_2 = (1 - a_1)(\varepsilon_1 + \delta_1) - (1 - a_2)(\varepsilon_2 + \delta_2)$.

For $T_{\mathrm{Dy}} < T < T_N$ the magnetoelastic distortion is absent [Fig. 2(b)], and the magnetic polarization at the Dy site is weak. Neutron diffraction [2] and Mössbauer [6] experiments give an upper limit of $0.1\mu_B$ for the ordered Dy $4f$ moment above T_{Dy}, so that for this temperature range we may remove assumption (ii), setting $\delta_1 = \delta_2 = 0$. The ratio A_1/A_2 then yields an estimate of 2.2 electrons for the occupancy of the lower band (the upper band taken to be empty), which is in good agreement with estimates based on band structure calculations of the $5d$ states [1]. We plot the ratio of the sum and difference of the two parameters, A_2 and A_1, normalized to an occupancy of two electrons, in Fig. 2(b). As anticipated, this quantity is close to unity above T_{Dy}; however, important deviations are seen below. These may be interpreted as due to the increase of δ_1, δ_2 driven by the increasing ordered component of the Dy $4f$ moment and concomitant magnetoelastic distortion. The latter is observed as a growing amplitude of charge scattering at the $2q$ satellites on cooling, the temperature dependence of which is indicated in Fig. 2(b). This hypothesis is supported by the thermal evolution of the band splitting parameter, g [inset to Fig. 2(b)], which has a form consistent with that expected for a system of magnetic Dy ions in the field of the ordered Fe ions ($T_{\mathrm{Dy}} < T < T_N$) and subject to a growing self-consistent molecular field on cooling. In addition to reproducing the intensity changes, the model accurately gives the energy dependencies (Fig. 3) as a function of temperature with no additional parameters.

The scope of the model may be increased by making the matrix elements dependent on band index, adding core level splitting, anisotropic occupation of orbital momentum states in the $5d$ band, and by removing restrictions on $\varepsilon_1, \varepsilon_2$. Such effects are unnecessary for a preliminary understanding; however, they are not excluded. Scattering amplitudes based on an energy splitting of spin-up–spin-down states, adapted to isolated ions or, possibly, ferromagnetic bands, have been considered [8–10,15,16]. In such cases a major difficulty arises since, while coefficient A_1 is, as in the antiferromagnetic case, proportional to the electronic polarization, A_2 becomes proportional to the total electron count in the shell. It is therefore expected to be temperature independent, which is difficult to reconcile with the present data.

The present experiments, which probe the polarization of the Dy $5d$ bands, are consistent with an initial ordering of these states in the field of the Fe ions, followed by a rapid increase in order below T_{Dy}. The anomalous thermal evolution of the scattering intensity and its dependence on incident photon energy are modeled taking into account the antiferromagnetic, metallic nature of the compound. We propose that changes in the radial matrix elements caused by the increasing ordered component of the Dy $4f$ moment and concomitant magnetoelastic distortion below T_{Dy} are responsible for the abnormal behavior of the L_3/L_2 intensity ratio. The similarity of the L_3/L_2 ratio at low T with that found in pure Dy supports the important role of $4f$ polarization on the radial matrix elements in the pure material [16].

We have shown that XRES, which is both element and electron-shell specific, may be used to gain information on $5d$ sublattice interactions through the positions and intensities of the resonant peaks.

Discussions with Mike Brooks of Karlsruhe and John Hill of BNL are much appreciated. The HCM EC funded training program partly funded S. L. and N. B., and the latter also thanks the ILL, Grenoble and ITE, Karlsruhe for financial support. J. A. P. acknowledges support from JNICT under Contract No. PRAXIS/FIS/2213/95. Work performed at Brookhaven is supported by U.S. DOE under Contract No. DE-AC02-98CH10886.

*Present address: Rutherford Appleton Laboratory, ISIS Facility, Chilton, Didcot, Oxon OX11 0QX, United Kingdom.

[1] J. Jensen and A. Mackintosh, *Rare-Earth Magnetism* (Clarendon Press, Oxford, 1991).
[2] J. A. Paixão *et al.* (to be published).
[3] J. A. Paixão *et al.*, Phys. Rev. B **55**, 14 370 (1997).
[4] K. H. J. Buschow and A. M. van der Kraan, J. Phys. F, Met. Phys. **8**, 921 (1978).
[5] W. Schäffer and G. Will, J. Less-Common Met. **94**, 205 (1983).
[6] P. C. M. Gubbens *et al.*, J. Magn. Magn. Mater. **27**, 61 (1982).
[7] A. Stunault *et al.*, J. Synchrotron Res. **5**, 1010 (1998).
[8] D. Gibbs *et al.*, Phys. Rev. Lett. **61**, 1241 (1988); J. P. Hannon *et al.*, *ibid.* **61**, 1245 (1988).
[9] D. Gibbs *et al.*, Phys. Rev. B **43**, 5663 (1991).
[10] P. Carra *et al.*, Phys. Rev. Lett. **66**, 2495 (1991).
[11] F. Bartolemé *et al.*, Phys. Rev. Lett. **79**, 3775 (1997).
[12] J. P. Hill and D. F. McMorrow, Acta Crystallogr. Sect. A **52**, 236 (1996).
[13] C. Herring, in *Magnetism*, edited by G. Rado and H. Suhl (Academic Press, New York, 1966), Vol. IV.
[14] M. Blume, J. Appl. Phys. **57**, 3615 (1985).
[15] J. Luo *et al.*, Phys. Rev. Lett. **71**, 287 (1993).
[16] M. van Veenendaal *et al.*, Phys. Rev. Lett. **78**, 1162 (1997).